ChemComm

Accepted Manuscript

This article can be cited before page numbers have been issued, to do this please use: Y. Shi, Y. Hu, G. Ochbaum, R. Lin, R. Bitton, H. Cui and H. S. Azevedo, *Chem. Commun.*, 2017, DOI: 10.1039/C7CC03512H.

ROYAL SOCIETY OF CHEMISTRY

rsc.li/chemcomm

View Article Online
DOI: 10.1039/C7CC03512H

Journal Name

COMMUNICATION

Enzymatic activation of cell-penetrating peptides in self-assembled nanostructures triggers fibre-to-micelle morphological transition†

Received 00th January 20xx,
Accepted 00th January 20xx

DOI: 10.1039/x0xx00000x

www.rsc.org/

Yejiao Shi[a], Yang Hu[b], Guy Ochbaum[c], Ran Lin[b], Ronit Bitton[c], Honggang Cui[b] and Helena S. Azevedo*[a]

We report here a proof-of-concept design of a multidomain cell-penetrating peptide amphiphile (CPPA) which can self-assemble into fibrous nanostructures and swtich to spherical micelles upon enzymatic degradation by the matrix metalloproteinase-2 (MMP-2) up-regulated in the tumour environment. Concomitant with this morphological transition, the cell-penetrating peptide (CPP), which was previously buried inside the CPPA fibers, could be presented on the surface of the CPPA micelles, enhancing their cell-penetrating ability. These multifunctional and enzyme-responsive CPP nanostructures hold potential as nanocarriers for tumour-targeted intracelllular delivery of therapeutic and diagnostic agents.

Cell-penetrating peptides (CPPs) are a family of short peptides that are capable of translocating across cell membranes effectively[1]. Since the discovery of the first CPP, more than two decades ago[2], CPPs have been widely used to enhance the intracellular delivery of diverse molecules and particles[3, 4], including chemotherapeutic drugs, peptides and proteins, nucleic acids, imaging agents, quantum dots and liposomes. Although the cellular uptake mechanism of CPPs is not fully understood, experimental evidences have shown that electrostatic interactions between the positively charged amino acid residues of CPPs and the negatively charged proteoglycans or glycosaminoglycans on the cell surface play an important role in the membrane translocation of CPPs, regardless of other possible mechanisms (endocytosis and macropinocytosis) involved[5]. However, the cationic property of CPPs also causes their non-selective electrostatic interactions with anionic biological molecules or membranes, leading to their poor tumour targeting ability[6]. To harness the power of CPPs for tumour-targeted delivery, a number of strategies have been developed to allow the *in situ* presentation of CPPs in response to endogenous disease conditions (pH, enzyme activities, redox potential) or locally applied exogenous stimuli (temperature, ultrasound, magnetic or electrical fields, light) only at the tumour site[7, 8]. However, the multiple functionalization steps involved in these strategies make both the preparation process and the final architectures complex. The design of multifunctional and stimuli-sensitive CPP nanostructures that could be formed in a single step would be highly desirable. This is where peptide self-assembly can make a contribution[9].

To deal with the aforementioned challenges, we designed a self-assembling cell-penetrating peptide amphiphile (CPPA) with multiple functional domains (Fig. S1): (i) a hydrophobic palmitic acid tail C_{16}, which could act as the hydrophobic driving force for self-assembly[10] and also provide the hydrophobic region for the entrapment of chemotherapeutic drugs[11, 12]; (ii) a CPP sequence YTA4 (IAWVKAFIRKLRKGPLG), which contains parts of the MMP-2 sensitive peptide sequence (GPLG)[13]. The cationic property of this CPP sequence adds amphiphilicity to the designed CPPA to favour its self-assembly and also enables the cell-penetrating ability of the assemblies; (iii) a MMP-2 sensitive octapeptide linker (GPLGIAGQ), which has been reported to be cleaved at the site between glycine (G) and isoleucine (I)[14] by MMP-2 that is overexpressed and activated in the tumour environment[15, 16], thus enabling the controlled presentation of CPP; and (iv) a targeting peptide moiety (RGDS), which could be specifically recognized by αvβ3 and αvβ5 integrins overexpressed on the surface of tumour cells[17]. It could act as a shelter for the off-targeted CPP sequence upon self-assembly and enable the specific tumour accumulation of the assemblies. We hypothesized that the rationally designed CPPA could self-assemble into defined nanostructures in aqueous environment, with the targeting moiety being presented on the surface and the CPP sequence being buried inside of the assemblies. The targeting moiety on the surface of the assemblies could protect the off-targeted CPP, while allowing the specific accumulation of the

[a] School of Engineering and Materials Science, Institute of Bioengineering, Queen Mary, University of London, London, E1 4NS, UK. E-mail: h.azevedo@qmul.ac.uk
[b] Department of Chemical and Biomolecular Engineering, Institute for NanoBioTechnology, Johns Hopkins University, Baltimore, MD 21218,USA
[c] Department of Chemical Engineering and the Ilza Katz, Institute for Nanoscale Science & Technology, Ben-Gurion University of the Negev, Beer-Sheva 84105, Israel

† Electronic Supplementary Information (ESI) available: See DOI: 10.1039/x0xx00000x

View Article Online
DOI: 10.1039/C7CC03512H

assemblies at the tumour site. The overexpression and activation of MMP-2 in the tumour environment could then initiate the cleavage of the MMP-2 sensitive linker and trigger the presentation of the CPP sequence to facilitate the penetration of the CPPA assemblies across the cell membranes.

Herein, the multi-domain self-assembling CPPA and its expected product from the MMP-2 enzymatic degradation ($CPPA_{MMP}$) were firstly synthesized and purified (Fig. S2 and S3, ESI†). Their self-assembly behaviour and structural properties were then investigated by circular dichroism (CD) and fluorescence spectroscopy, transmission electron microscopy (TEM) and small angle X-ray scattering (SAXS).

The amphiphilicity of CPPA offers an opportunity to drive its self-assembly process. Using a sovatochromic fluorescence dye, Nile Red, which exhibits an increased fluorescence intensity and pronounced blue shift when encapsulated into the hydrophobic region of self-assembled nanostructures[18], the critical aggregation concentration (CAC) of CPPA was determined at 0.02 mM (Fig. 1A).

To further characterize the structural properties of the CPPA assemblies, TEM together with SAXS were used to analyse their shape and size. As displayed in Fig. 1B, TEM observation revealed the formation of fibrous structures with a micron scale length and a roughly 18 nm diameter. This observation was confirmed by SAXS (Fig. 1C), which yielded a slope of -1, indicating the formation of cylindrical nanostructures. A polydisperse core-shell cylinder fit was applied to these cylindrical nanostructures and a diameter of 2.3 ± 0.2 nm was calculated. The hydrodynamic diameter calculated from SAXS is mainly for the hydrophobic core of the CPPA fibres and therefore a smaller value was obtained compared to the mean diameter measured by TEM.

To investigate the enzyme responsiveness of the CPPA assemblies, CPPA fibres were incubated with active MMP-2 at 37 °C and their cleavability was monitored over time by analytical RP-HPLC. As demonstrated in Fig. 2, at the starting point of incubation, only one peak was shown in the HPLC chromatogram, corresponding to the uncleaved CPPA. With increasing incubation time, the CPPA peak decreased, while an increasing new peak with longer retention time was observed. The extended retention time indicates the presence of a less polar product. ESI-MS analysis of the fraction collected from the increasing new peak showed a mass that corresponds to the expected peptide fragment after the MMP-2 degradation (Fig. S4, ESI†). In contrast, when CPPA fibres were incubated alone, without the active MMP-2 enzyme, no change was detected over time. These results suggested that the CPPA fibres can be fully cleaved by MMP-2, even though the MMP-2 sensitive peptide sequence was conjugated with both CPP and targeting sequences at its two ends and buried inside the CPPA fibres. Our design on the controlled presentation of CPP upon degradation by MMP-2 was proved to be practical.

Upon enzymatic degradation, the shorter cleaved segment is released from the assemblies and the fine balance among the multiple intermolecular forces that hold the assemblies might be disturbed. As a consequence, a change in the self-assembly behaviour could be triggered. Previous studies have reported the dissociation of self-assembled structures upon MMP degradation. For example, Hartgerink and co-workers have designed self-assembling multi-domain peptide based hydrogels that contained an MMP-2-specific cleavable domain. Enzyme-mediated digestion and collapse of the hydrogel was observed due to the disruption of the nanofibrous network[19]. Chau *et al.* have incorporated the MMP-2 sensitive sequence into self-assembling[20] peptides for generating enzyme degradable nanofibrous scaffold hydrogels that could mimic the remodelling of natural extracellular matrix during tissue regeneration[21]. Cui's lab has also used the MMP-2 peptide substrate for designing degradable peptide-based supramolecular filaments[22]. On the other hand, Xu's group has provided compelling evidence that the MMP-9 enzyme could

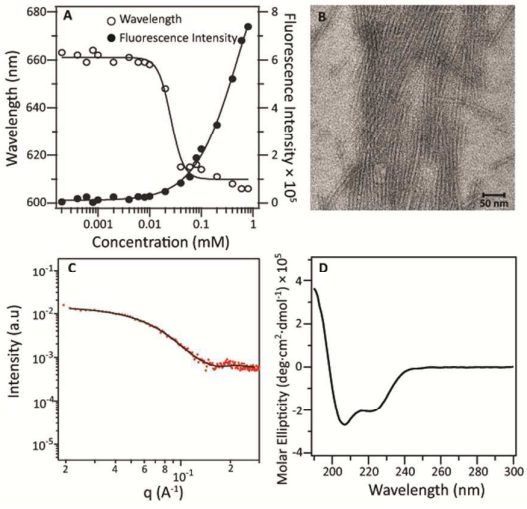

Fig. 1 Self-assembly behaviour of CPPA in Milli-Q water, pH 7.4: (A) maximum fluorescence emission wavelength and intensity of Nile Red as a function of CPPA concentration to determine the CAC of CPPA; (B) representative TEM image of CPPA (200 μM) showing fibrous nanostructures; (C) SAXS profile fitted with a core-shell cylinder model for CPPA (2 mM); (D) CD spectrum of CPPA (50 μM) indicating α-helix secondary structure.

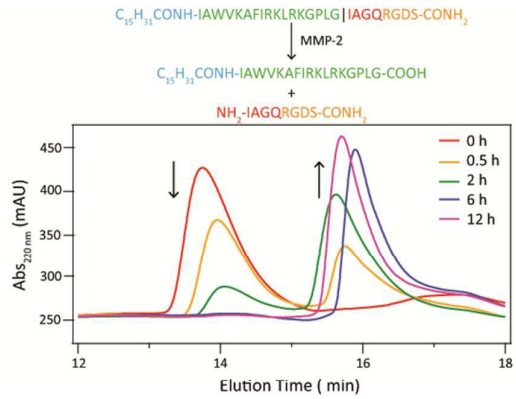

Fig. 2 MMP-2 responsiveness of CPPA fibers: analytical RP-HPLC traces of 200 μM CPPA incubated with 20 nM active MMP-2 in TCNB buffer at 37 °C for different time intervals.

View Article Online
DOI: 10.1039/C7CC03512H

trigger the formation, instead of dissociation, of a short peptide based supramolecular hydrogel[23]. A micelle-to-fibre morphological transition of palmitylated PAs, induced by MMP-7, has been previously reported by Koda *et al*[24] and the same morphological transition was accomplished via MMP-9 cleavage of the phenylacetyl PAs designed by Ulijn's group[25].

Therefore, we further investigated whether the fibrous structure of the CPPA assemblies could be maintained after the enzymatic degradation by MMP-2. For this purpose, the self-assembly behaviour and structural properties of $CPPA_{MMP}$ were characterized. As shown in Fig. 3, $CPPA_{MMP}$ still hold the self-assembly ability, but a higher CAC of 0.08 mM is required to drive the self-assembly process. TEM imaging of $CPPA_{MMP}$ showed the formation of spherical micelles with a 20 nm diameter. The spherical morphology was further confirmed by SAXS, which yielded a slope of 0, indicating the presence of spherical micelles. A polydisperse core-shell sphere fit was applied to these spherical nanostructures and a diameter of 2.9 ± 0.3 nm was calculated. These observations suggest that the designed CPPA can self-assemble into fibres in aqueous solution and reconfigure to spherical micelles upon MMP-2 degradation. This fibre-to-micelle morphological transition offers an attractive method for the systemic delivery of therapeutic and diagnostic agents intracellularly. Following systemic delivery, fibrous structures are preferred over spherical counterparts as filamentous structures have been previously reported to remain in circulation 10 times longer than spherical particles[26]. A recent work developed at the Stupp's lab also demonstrated that cylindrical nanostructures have the capacity of targeting injured blood vessels following systemic delivery, while spherical micelles with comparable diameter failed to bind[27]. However, spherical structures with relatively smaller and uniform size are more appealing over fibrous structures when considering the cell internalization efficiency[20, 28].

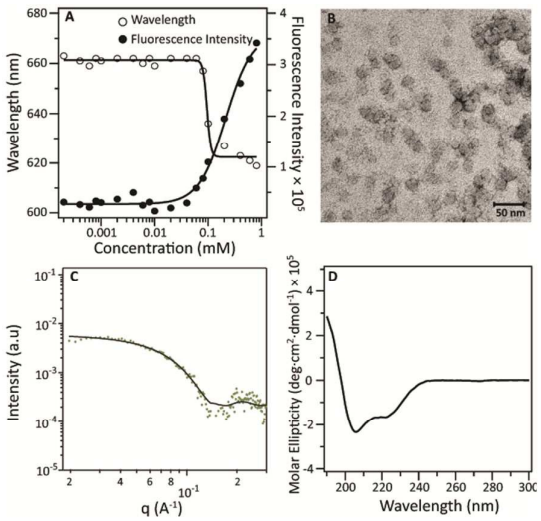

Fig. 3 Self-assembly behaviour of $CPPA_{MMP}$ in Milli-Q water, pH 7.4: (A) maximum fluorescence emission wavelength and intensity of Nile Red as a function of $CPPA_{MMP}$ concentration to determine the CAC of $CPPA_{MMP}$; (B) representative TEM image of $CPPA_{MMP}$ (200 μM) showing spherical micelle nanostructures; (C) SAXS profile fitted with a core-shell micelle model for $CPPA_{MMP}$ (2 mM); (D) CD spectrum of $CPPA_{MMP}$ (50 μM) indicating α-helix secondary structure.

To better understand the fibre-to-micelle morphological transition, secondary structure of CPPA and $CPPA_{MMP}$ was studied as it plays a significant role in the self-assembly of PAs[29, 30]. PAs with a β-sheet secondary structure typically yield elongated micelles due to the strong hydrogen bonding among the peptides that bring them close together, minimizing the curvature of the micelles[10]. On the other hand, PAs with a α-helix secondary structure usually form spherical micelles[29, 31], even though elongated micelles have also been observed[32, 33]. In particular, previous work by Tirrell's group has demonstrated that assembled PA micelles undergo a spherical to cylindrical morphology transition over time with a switch in the secondary structure from α-helix to β-sheet[34]. However, CD spectra shown in Fig 1D and 3D revealed that both CPPA and $CPPA_{MMP}$ have an α-helix secondary structure at physiological pH. It is likely that, in addition to the hydrogen bonding, the electrostatic and steric forces could also affect the inter-peptide interactions and folding, contributing to the final morphology of the assemblies[27, 35, 36]. In the CPPA, the peptide interactions of the α-helix conformation are strong enough to hold them together tightly, resulting in fibrous nanostructures. However, the presence of charged side groups from lysine and arginine, at one end of the $CPPA_{MMP}$ sequence generate electrostatic repulsion forces, instead of cohesive forces, contributing to the formation of looser core-shell spherical micelles.

In order to verify our hypothesis, that the CPP sequence could be shielded inside the assemblies by the MMP-2 sensitive and targeting sequences upon self-assembly, zeta-potential measurements were performed. As expected, a lower zeta-potential for CPPA fibres (62.8±0.3 mV) was obtained compared to that of $CPPA_{MMP}$ spherical micelles (81.8±1.4 mV) at physiological pH in Milli-Q water, confirming that upon self-assembly, CPP sequence can be buried inside the assemblies and its positive charges can be partly shielded by the MMP-2 sensitive and targeting sequences.

In summary, we report here a proof-of-concept design of a multi-domain CPPA that can self-assemble into fibres in aqueous environment. The fibrous structure of the CPPA assemblies has a potential to prolong their circulation time in the blood stream. At the same time, active tumour accumulation could be achieved by the targeting moiety, which can also steric shield the CPP sequence and prevent the non-specific intracellular uptake of the CPPA fibres. Upon accumulation in the tumour environment, the overexpressed MMP-2 can cleave its sensitive linker, resulting in the detachment of the protective targeting moiety and exposing the previously hidden CPP sequence on the surface of the CPPA assemblies to facilitate the cell-penetrating process. Compared with conventional designs, the proposed multifunctional and enzyme-sensitive CPP nanostructures can be easily synthesized and fabricated via self-assembly. Their unique fibre-to-micelle morphological transition and controlled CPP presentation properties offer a greater possibility to achieve enhanced tumour cell targeting and

View Article Online
DOI: 10.1039/C7CC03512H

penetrating. However, we are conscious that there are still several challenges ahead to optimize these CPP nanostructures for *in vivo* applications. First and foremost, the CAC value of the CPP nanostructures must be reduced to the nanomolar range to keep stable nanostructures during circulation[37]. Second, longer targeting peptide sequences or polymers may be needed to completely block the function of the CPP sequence. In our current design, although the CPP sequence could be shielded by the targeting moiety, as demonstrated by the decreased zeta-potential value, the positive charge of the CPPA fibres is still too high. Nonetheless, we demonstrated a valuable design for developing multifunctional and enzyme-responsive CPP nanostructures with a greater possibility to achieve enhanced tumour accumulation and intracellular delivery of therapeutic and diagnostic. Further optimization of this CPPA design and *in vitro* evaluation of the CPP nanostructures are on-going in our lab.

Acknowledgements

Y. Shi thanks the China Scholarship Council for providing her a PhD Scholarship (No.201307060020) and the Postgraduate Research Fund from Queen Mary, University of London for supporting her short-term visit to Johns Hopkins University.

Notes and references

1. F. Milletti, *Drug discovery today*, 2012, **17**, 850-860.
2. A. D. Frankel and C. O. Pabo, *Cell*, 1988, **55**, 1189-1193.
3. E. Koren and V. P. Torchilin, *Trends in molecular medicine*, 2012, **18**, 385-393.
4. F. Wang, Y. Wang, X. Zhang, W. Zhang, S. Guo and F. Jin, *Journal of controlled release*, 2014, **174**, 126-136.
5. D. M. Copolovici, K. Langel, E. Eriste and U. Langel, *ACS nano*, 2014, **8**, 1972-1994.
6. N. Q. Shi, X. R. Qi, B. Xiang and Y. Zhang, *Journal of controlled release*, 2014, **194**, 53-70.
7. Y. Huang, Y. Jiang, H. Wang, J. Wang, M. C. Shin, Y. Byun, H. He, Y. Liang and V. C. Yang, *Advanced drug delivery reviews*, 2013, **65**, 1299-1315.
8. S. R. MacEwan and A. Chilkoti, *Wiley interdisciplinary reviews. Nanomedicine and nanobiotechnology*, 2013, **5**, 31-48.
9. M. S. Ekiz, G. Cinar, M. A. Khalily and M. O. Guler, *Nanotechnology*, 2016, **27**, 402002.
10. H. Cui, M. J. Webber and S. I. Stupp, *Biopolymers*, 2010, **94**, 1-18.
11. M. O. Guler, R. C. Claussen and S. I. Stupp, *J Mater Chem*, 2005, **15**, 4507-4512.
12. P. Zhang, A. G. Cheetham, Y. A. Lin and H. Cui, *ACS nano*, 2013, **7**, 5965-5977.
13. M. Lindgren, K. Rosenthal-Aizman, K. Saar, E. Eiriksdottir, Y. Jiang, M. Sassian, P. Ostlund, M. Hallbrink and U. Langel, *Biochem Pharmacol*, 2006, **71**, 416-425.
14. H. Nagase and G. B. Fields, *Peptide Science*, 1996, **40**, 399-416.
15. C. M. Overall and O. Kleifeld, *Nature reviews. Cancer*, 2006, **6**, 227-239.
16. B. Schmalfeldt, D. Prechtel, K. Harting, K. Spathe, S. Rutke, E. Konik, R. Fridman, U. Berger, M. Schmitt, W. Kuhn and E. Lengyel, *Clinical cancer research*, 2001, **7**, 2396-2404.
17. E. Ruoslahti, *Annual review of cell and developmental biology*, 1996, **12**, 697-715.
18. M. C. A. Stuart, J. C. van de Pas and J. B. F. N. Engberts, *J Phys Org Chem*, 2005, **18**, 929-934.
19. K. M. Galler, L. Aulisa, K. R. Regan, R. N. D'Souza and J. D. Hartgerink, *Journal of the American Chemical Society*, 2010, **132**, 3217-3223.
20. H. Cabral, Y. Matsumoto, K. Mizuno, Q. Chen, M. Murakami, M. Kimura, Y. Terada, M. R. Kano, K. Miyazono, M. Uesaka, N. Nishiyama and K. Kataoka, *Nature nanotechnology*, 2011, **6**, 815-823.
21. M. C. Giano, D. J. Pochan and J. P. Schneider, *Biomaterials*, 2011, **32**, 6471-6477.
22. Y. A. Lin, Y. C. Ou, A. G. Cheetham and H. Cui, *Biomacromolecules*, 2014, **15**, 1419-1427.
23. Z. Yang, M. Ma and B. Xu, *Soft Matter*, 2009, **5**, 2546-2548.
24. D. Koda, T. Maruyama, N. Minakuchi, K. Nakashima and M. Goto, *Chemical communications*, 2010, **46**, 979-981.
25. D. Kalafatovic, M. Nobis, N. Javid, P. W. Frederix, K. I. Anderson, B. R. Saunders and R. V. Ulijn, *Biomaterials science*, 2015, **3**, 246-249.
26. Y. Geng, P. Dalhaimer, S. Cai, R. Tsai, M. Tewari, T. Minko and D. E. Discher, *Nature nanotechnology*, 2007, **2**, 249-255.
27. T. J. Moyer, H. A. Kassam, E. S. Bahnson, C. E. Morgan, F. Tantakitti, T. L. Chew, M. R. Kibbe and S. I. Stupp, *Small*, 2015, **11**, 2750-2755.
28. K. Huang, H. Ma, J. Liu, S. Huo, A. Kumar, T. Wei, X. Zhang, S. Jin, Y. Gan, P. C. Wang, S. He, X. Zhang and X. J. Liang, *ACS nano*, 2012, **6**, 4483-4493.
29. A. Trent, R. Marullo, B. Lin, M. Black and M. Tirrell, *Soft Matter*, 2011, **7**, 9572-9582.
30. S. R. Bull, M. O. Guler, R. E. Bras, T. J. Meade and S. I. Stupp, *Nano letters*, 2005, **5**, 1-4.
31. F. Boato, R. M. Thomas, A. Ghasparian, A. Freund‐Renard, K. Moehle and J. A. Robinson, *Angewandte Chemie International Edition*, 2007, **46**, 9015-9018.
32. S. M. Standley, D. J. Toft, H. Cheng, S. Soukasene, J. Chen, S. M. Raja, V. Band, H. Band, V. L. Cryns and S. I. Stupp, *Cancer research*, 2010, **70**, 3020-3026.
33. D. Missirlis, M. Farine, M. Kastantin, B. Ananthanarayanan, T. Neumann and M. Tirrell, *Bioconjugate chemistry*, 2010, **21**, 465-475.
34. T. Shimada, S. Lee, F. S. Bates, A. Hotta and M. Tirrell, *The journal of physical chemistry. B*, 2009, **113**, 13711-13714.
35. A. Ghosh, E. T. Dobson, C. J. Buettner, M. J. Nicholl and J. E. Goldberger, *Langmuir,* 2014, **30**, 15383-15387.
36. T. J. Moyer, J. A. Finbloom, F. Chen, D. J. Toft, V. L. Cryns and S. I. Stupp, *Journal of the American Chemical Society*, 2014, **136**, 14746-14752.
37. L. L. Lock, A. G. Cheetham, P. Zhang and H. Cui, *ACS nano*, 2013, **7**, 4924-4932.